ANALYSIS MARS

Assessment of Mars Exploration Rover landing site predictions

M. P. Golombek[1], R. E. Arvidson[2], J. F. Bell III[3], P. R. Christensen[4], J. A. Crisp[1], L. S. Crumpler[5], B. L. Ehlmann[6], R. L. Fergason[4], J. A. Grant[7], R. Greeley[4], A. F. C. Haldemann[1], D. M. Kass[1], T. J. Parker[1], J. T. Schofield[1], S. W. Squyres[3] & R. W. Zurek[1]

Comprehensive analyses of remote sensing data during the three-year effort to select the Mars Exploration Rover landing sites at Gusev crater and at Meridiani Planum correctly predicted the atmospheric density profile during entry and descent and the safe and trafficable surfaces explored by the two rovers. The Gusev crater site was correctly predicted to be a low-relief surface that was less rocky than the Viking landing sites but comparably dusty. A dark, low-albedo, flat plain composed of basaltic sand and haematite with very few rocks was expected and found at Meridiani Planum. These results argue that future efforts to select safe landing sites based on existing and acquired remote sensing data will be successful. In contrast, geological interpretations of the sites based on remote sensing data were less certain and less successful, which emphasizes the inherent ambiguities in understanding surface geology from remotely sensed data and the uncertainty in predicting exactly what materials will be available for study at a landing site.

Selection of the Mars Exploration Rover (MER) landing sites took place over a three-year period in which engineering constraints were identified, of 155 possible sites two were selected, surface environments and safety considerations were developed, and the potential scientific knowledge to be obtained at the sites was considered[1]. Landing sites in the Gusev crater and at Meridiani Planum were selected because they appeared acceptably safe for MER landing and roving and had strong morphologic or mineralogical indicators of having had liquid water in the past. The two sites therefore appeared capable of addressing the science objectives of the MER missions: to determine the aqueous, climatic and geologic history of sites on Mars where conditions may have been favourable to the preservation of evidence of possible pre-biotic or biotic processes.

Engineering constraints important to the selection included: latitude (10° N–15° S) for maximum solar power; elevation (<−1.3 km) for sufficient atmosphere to slow the descent of the lander; low horizontal winds, shear and turbulence in the last few kilometres to minimize horizontal velocity; low 10-m-scale slopes to reduce airbag spin-up and bounce; low to moderate rock abundance to reduce abrasion or stroke-out of the airbags; and a radar-reflective, load-bearing surface that is not dominated by fine-grained dust, and is thus safe for landing and roving[1]. In selecting the MER landing sites these engineering constraints were addressed via comprehensive evaluation of surface and atmospheric characteristics from existing remote sensing data and models as well as targeted orbital information acquired from the Mars Global Surveyor (MGS) and Mars Odyssey.

This evaluation resulted in a number of predictions of the surface characteristics of the sites[1], which are tested in this paper. Relating remote sensing signatures to surface characteristics at landing sites allows these sites to be used as ground truth for the orbital data, is essential for selecting and validating landing sites for future missions, and is required for correctly interpreting the surfaces and materials globally present on Mars.

General predictions

General predictions of the surface characteristics made before landing were that both landing sites would be safe for the MER landing system and traffickable by the rovers[1]. At Gusev crater, the available data suggested its appearance would be generally similar to the Viking Lander (VL) and Mars Pathfinder (MPF) landing sites, roughly as dusty but less rocky (Fig. 1). The geologic setting of the flat-floored Gusev crater at the end of Ma'adim Vallis, one of the largest branching valley networks on the planet, argued strongly that the materials inside were deposited in a crater lake[2,3]. The Late Hesperian/Early Amazonian cratered plains[3] upon which the landing site was principally sited showed little to reveal their origin with volcanic, aeolian (wind-formed) and lacustrine (lake-deposited) sedimentary materials as possibilities. If the surface materials were not lacustrine, it was hoped that the impacts would provide access to deeper materials that were[1].

At Meridiani Planum, the available data suggested a low-albedo surface with few rocks and little dust that would look completely unlike any of the VL or MPF landing sites[1] (Fig. 2). Evaluation of the geologic setting of Meridiani suggested a flat to gently rolling plain composed of basaltic sand with haematite and sparse outcroppings of a thin bright layer[4–6]. The identification of coarse-grained haematite in MGS Thermal Emission Spectrometer (TES) spectra and the geologic setting from Thermal Emission Imaging System (THEMIS) data argued for direct precipitation of haematite from highly oxygenated iron-rich lake waters, or via alteration by percolating fluids after burial[5,6] although alternative explanations were also possible[1].

All of the predictions of the general physical characteristics of the surface appear correct in the exploration of the landing sites by the rovers. In addition, we have compared the specific remote sensing data at the same landing and traverse locations[7,8] to the surface characteristics observed by the rovers. The predictions of the materials that would be found scientifically at the two landing sites have proved less definitive.

[1]Jet Propulsion Laboratory, California Institute of Technology, Pasadena, California 91109, USA. [2]Washington University, St Louis, Missouri 63130, USA. [3]Cornell University, Ithaca, New York 14853, USA; [4]Arizona State University, Tempe, Arizona 85287, USA. [5]New Mexico Museum of Natural History and Science, Albuquerque, New Mexico 87104, USA. [6]Oxford University, OX1 3PG, UK; [7]Smithsonian Institution, Washington DC 20560, USA.

Atmosphere

Although the atmosphere (density and winds, in particular) was a key concern for safely landing the MER rovers[9], there was no instrumentation to measure the atmosphere encountered directly. An advisory team was assembled to assess the available information in a timely manner, especially for Spirit (Opportunity would land three weeks later). In the case of the density (pressure and temperature), the deceleration profile was useful to reconstruct the atmosphere (as was done for Pathfinder[10]). A temperature profile was obtained with simple assumptions from a density profile derived from the deceleration curve and aeroshell drag properties.

A preliminary reconstruction immediately after landing was within the one-standard-low-deviation uncertainty bounds of the a priori atmosphere model[1] through most of the descent (as adjusted for the December 2003 dust storm using MGS TES temperature profiles[11] just before landing) for both Spirit and Opportunity. The mean model temperatures were within ~5 K of the preliminary reconstructed profile throughout the atmosphere for Spirit, with the model being warm below ~15 km and cool between 20 and 35 km. The Opportunity model showed a similar pattern of differences, but the deviations were as large as ~15 K (although the reconstructed profile was more uncertain). Both models overestimated the mean densities by an average of 8% throughout the atmosphere owing to uncertainties below 5 km. The MGS Mars Orbiter Laser Altimeter (MOLA)[12] elevations that were used to construct the density profiles are in excellent agreement with the elevations determined via radio tracking (within 7 m for Spirit and <1 m for Opportunity), thereby providing an accurate reference for the atmospheric model[9].

Determining the wind and wind shear that the flight system encountered during descent is extremely difficult (the response has to be separated from other effects and the intrinsic flight system behaviour). It appears that the winds encountered were within the expectations based on the modelling. In a qualitative sense it seems that the Meridiani landing site was less windy than at the Gusev crater, as expected[9]. There is some evidence that both landers were in an updraft during the last few kilometres, but this is not surprising given that the modelling predicted ~40% of the area would be experiencing updrafts at both sites[9]. Perhaps the most basic measure of the atmospheric modelling success is that both landers arrived safely and that the backshell rocket systems[1,13] on each spacecraft (added partly on account of atmospheric concerns) were both critical to ensuring a safe landing (without them, the Spirit landing in the Gusev crater would have been very close to the limit of the airbag performance envelope).

Thermal inertia

Thermal inertia is a measure of the resistance of surface materials to a change in temperature and can be related to particle size, bulk density and cohesion[14]. Surfaces dominated by loose dust have lower thermal inertia and typically high albedo, whereas those dominated by rock or duricrust (cemented soil-like materials) have higher thermal inertia. The fine-component thermal inertia is the thermal inertia of the surface after the thermal radiance attributable to the rocky component is factored out[15].

Orbital thermal inertia measurements of both landing sites[16–18] suggested surfaces that are competent and load bearing (without thick deposits of fine-grained dust) that pose no special risk to landing or roving[1]. The landing location in Gusev crater has a bulk TES thermal inertia of 315 $J\,m^{-2}\,s^{-0.5}\,K^{-1}$, which is consistent with the Viking[17]- and THEMIS[5,18]-derived thermal inertias (284 and 306 $J\,m^{-2}\,s^{-0.5}\,K^{-1}$, respectively). These thermal inertias suggested the surfaces are dominated by duricrust or cohesionless sand or granules[19,20], which is consistent with observed soil characteristics[21] and Mini-TES measured thermal inertias (150–430 $J\,m^{-2}\,s^{-0.5}\,K^{-1}$) from the surface[22]. Average THEMIS thermal inertia along the traverse at the Gusev crater (Fig. 3) varies from 285 $J\,m^{-2}\,s^{-0.5}\,K^{-1}$ at the landing site, to 290 $J\,m^{-2}\,s^{-0.5}\,K^{-1}$ part of the way up the

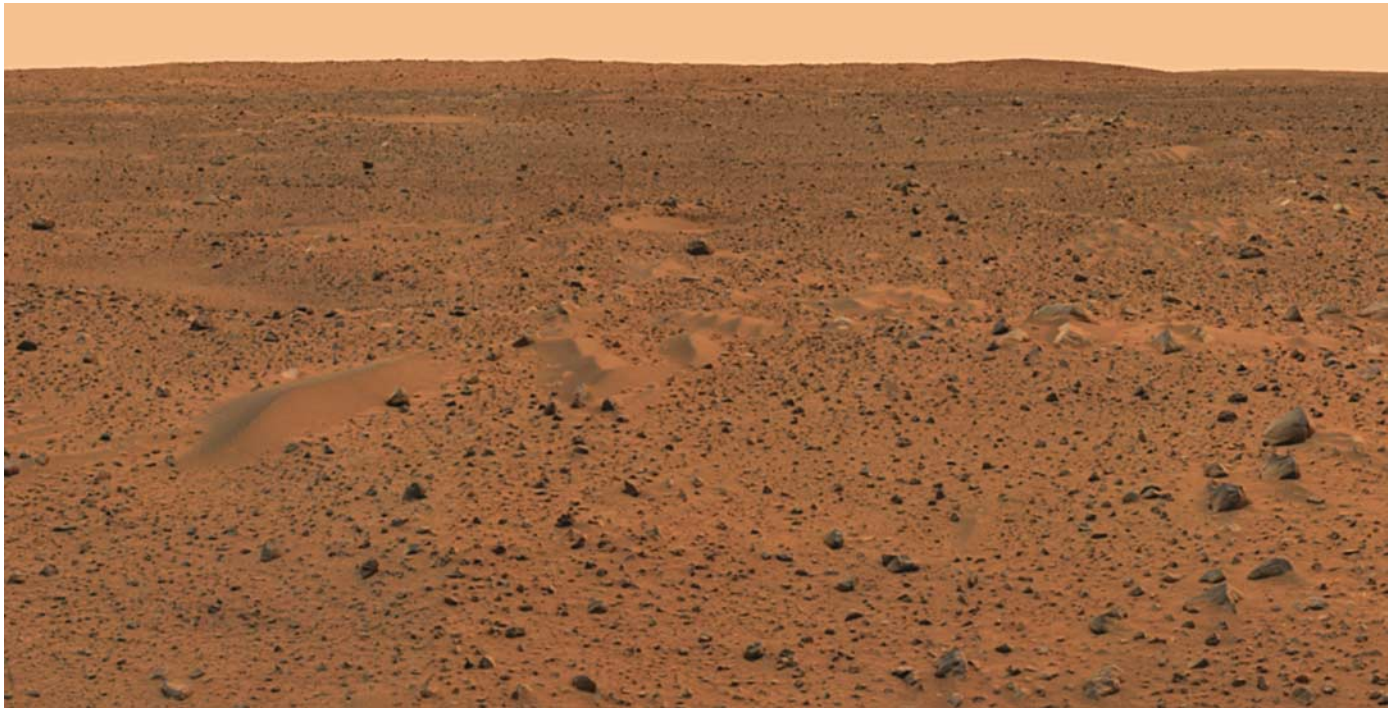

Figure 1 | Portion of the panorama obtained from the Spirit landing site, showing the moderately rocky, relatively smooth plain predicted from remotely sensed data. The bright region on the horizon is the brighter and dustier Bonneville crater rim, which is characteristic of most of the landing ellipse, as opposed to the lower-albedo and less-dusty landing location in a dust devil track. We note filled-in impact craters (circular hollows) and dark drifts and the pebble-rich surface, consistent with a dark armoured lag or pavement that has relatively little dust. Rock counts from the lander are from this area. This is an approximately true-colour rendering generated from a composite of images acquired through Pancam's 750-nm, 530-nm and 480-nm filters as part of imaging sequences P2215 and P2216 acquired on Spirit sols 4 and 5 (7 and 8 January 2004).

Bonneville ejecta, to 330 J m^{-2} s$^{-0.5}$ K^{-1} around Bonneville, and show systematic variations that can be related to observed variations in rock abundance and material properties[22,23].

In contrast, the landing location in Meridiani has TES and THEMIS bulk inertias of 200 and 190 J m^{-2} s$^{-0.5}$ K^{-1}, respectively, although Viking inertias are slightly higher (~315 J m^{-2} s$^{-0.5}$ K^{-1}). The TES and THEMIS inertias are similar to the Mini-TES measured inertias of 225 J m^{-2} s$^{-0.5}$ K^{-1} and correspond to surfaces dominated by 0.2-mm sand particles[20], which is consistent with the ubiquitous fine sand observed at Meridiani[24] (Fig. 2).

Albedo and dustiness

Spirit landed in the lowest-albedo portion of the Gusev landing ellipse characterized by dark dust-devil tracks (Fig. 3). As a result, the surface observed at the landing site is substantially less dusty than inferred for the rest of the ellipse. The average TES albedo[16] of the Gusev ellipse is ~0.23 and bright areas have albedos as high as 0.26. The low-albedo portion of the ellipse in the dust-devil track region in which Spirit landed has a much lower TES albedo of ~0.19, comparable to the Pancam surface measurement[25] (0.20), which is lower than the VL and MPF landing sites. The surface observed by Spirit at the landing site is characterized by a reddish soil surface with many dark granules, pebbles and small rocks as a lag or pavement (Fig. 1) and only modest amounts of bright atmospheric dust coating the rocks and soil surfaces, consistent with the lower albedo and the low dust index for this portion of the ellipse[26]. The albedos of bright areas like the rim of Bonneville crater that Spirit traversed into are much higher (0.30), consistent with orbital measurements of non-dust-devil track areas.

The average albedo of the Meridiani landing site in orbital data[16] is ~0.15 and thus it represents the first landing in a characteristically low-albedo portion of Mars[27]. Opportunity landed in an area of the ellipse with even lower albedo (~0.12) and the dust index of this part of the ellipse is among the lowest on Mars[26]. The dark sand-rich and dust-free surface observed on the Meridiani plains is consistent with its low albedo (Fig. 2). The brighter rim of the Eagle crater observed in the orbital and descent images is consistent with bright outcrops and brighter red soil surfaces that Opportunity has observed near the Eagle crater rim (Fig. 2). Pancam surface measurements[27] yield comparable albedos of 0.12 on the dark plains and higher albedos for the outcrops (0.25) and brighter wind streaks (0.19 to 0.29). The consistency between orbital and surface albedos and the presence or absence of bright dust further supports the use of albedo as a proxy for the dustiness of surfaces on Mars.

Figure 2 | Image of the Meridiani plain showing its dark, relatively dust- and rock-free plain, as predicted by orbital remote sensing data. The backshell, which is about 1 m high, and the parachute are about 450 m from the rover and illustrate the exceptionally smooth, flat and rock-free plain (except for the bright crater rim in the foreground), which was as predicted before landing. This is an approximately true-colour rendering generated from a composite of images acquired through Pancam's 750-nm, 530-nm and 430-nm filters as part of imaging sequence P2379 acquired on Opportunity sol 21 (14 February 2004).

Rock abundance

The average rock abundance of the Meridiani ellipse is ~5% as estimated from thermal differencing of the Viking Infrared Thermal Mapper (IRTM) data[15]. Rock abundance at the Gusev ellipse is higher (~7%) and similar to the global mode of ~8%. Opportunity landed at a location near the border of of 1% and 6% rock-abundance pixels (1° latitude and longitude) indicating[15] a rock abundance of a few per cent. Spirit is in an 8%-rock-abundance pixel and is not in portions of the ellipse where dense boulder fields were identified in MOC images[28]. These estimates suggested moderate rock abundance at the Gusev crater and very few rocks at Meridiani Planum, both of which have been relatively benign for driving the rover, as expected.

Rocks greater than ~0.04 m in diameter were counted within three roughly 70° sections of panoramas within 10 m of Spirit at the landing site (Mission Success), part of the way up the ejecta (Legacy), and at the rim of Bonneville crater (Bonneville), which have increasing bulk thermal inertias (Fig. 3). Results show that 7%, 5% and 29% of the surface is covered by rocks greater than ~0.04 m in diameter (Fig. 4) at these three sites, respectively. The size-frequency distribution of larger rocks (>0.1 m in diameter) generally follows the exponential model distribution based on the VL and MPF landing sites[28] for total rock abundances of 5%, 7% and 35% at the three respective sites, although there are far more pebbles at the Spirit landing site (consistent with less bright dust and drift material at this site) than at other locations. The largest rock size increases as the rock abundance increases, from 0.5 m to 0.8 m to 1.3 m in diameter towards the rim of Bonneville crater. Adjusting the intermediate rock count upward to account for the difference in bulk thermal inertia for this location versus the average (290 versus 306 J m^{-2} s$^{-0.5}$ K^{-1}) (assuming that the difference is due to more rocks)[23,28], about 7% of the surface would be covered by rocks more than 0.1 m in diameter, which compares favourably with the IRTM rock abundance[15] estimate of 8%. For effective thermal inertias of rock populations[28], the increase in bulk inertia on the Bonneville ejecta blanket is more than explained by the increase in rock

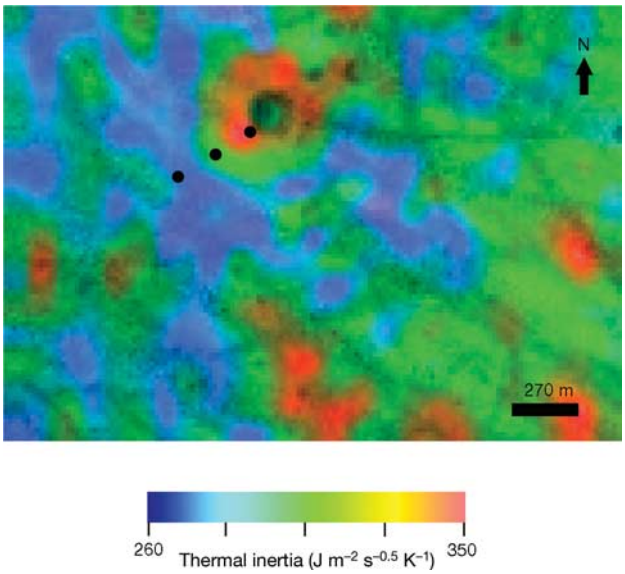

Figure 3 | THEMIS thermal inertia image in colour overlaid on a THEMIS visible image of Spirit landing area. It shows low-albedo, low-thermal-inertia intercrater plains where Spirit landed and locations with higher inertias on the drive to the rim of Bonneville crater where two other full Pancam panoramas[25] were acquired. Thermal inertia increases from 270 to 345 J m^{-2} s$^{-0.5}$ K^{-1} over this traverse with rock size-frequency distributions (reported in Fig. 4) at these three locations. The southwesternmost black dot is the Mission Success panorama where Spirit landed, the middle black dot is the Legacy panorama part of the way through the ejecta blanket, and the northeasternmost black dot is the rim of the Bonneville crater.

abundance, and suggests a corresponding decrease in the fine-component inertia, which appears consistent with observations of more dust closer to the rim.

The Meridiani plain is effectively devoid of rocks (Fig. 2) and Opportunity is the first lander to sample an area of Mars with very low rock abundance[15]. The orbital rock abundance estimate at this site is probably due to the outcrop, which appears to cover roughly 5% of the area within the ~20-m-diameter Eagle crater, and is exposed in crater interiors and rims and in fractures across the plain. In general, the area covered by outcrops and the rock-free plain appears consistent with the orbital estimate of several per cent of the surface covered by rocks at Meridiani Planum.

Slopes

Slopes were evaluated at three length scales important for landing[1]: 1 km, 100 m (from MOLA topography) and ≤10 m (from Mars Orbiter Camera stereogrammetry and photoclinometry). At all three scales Meridiani Planum is extraordinarily smooth and flat. From Opportunity's traverse telemetry[8] the root-mean-square (r.m.s.) slopes at these three scales are 0.3°, 0.7° and 1.4°, respectively, and follow a self-affine behaviour with a Hurst exponent[29] of 0.64. These slopes are consistent with the slopes reported before landing[1,30,31] and the exceptionally smooth and flat plain traversed by Opportunity (Fig. 2). The Gusev crater surface appeared rougher than the Meridiani plain, but smoother than VL1 and MPF in orbital data[1,30,31], which is consistent with the derived r.m.s. slopes from Spirit of 0.5°, 1.4°, and 2.5° at these three length scales (Hurst exponent of 0.58) and the relatively low-relief plain traversed by Spirit (Fig. 1).

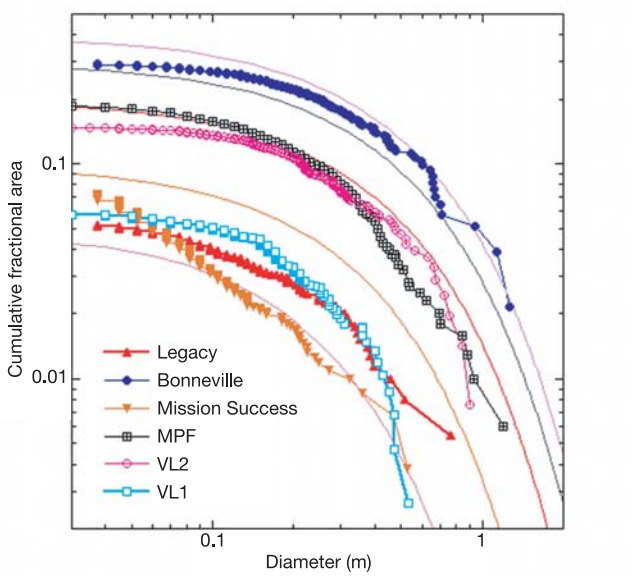

Figure 4 | Rock size-frequency distributions at three locations along the Spirit traverse, VL1, VL2 and MPF landing sites. Locations along the Spirit traverse are shown in Fig. 3. Solid lines are exponential cumulative fractional area versus diameter models[28] for 5%, 10%, 20%, 30% and 40% rock abundance (denoted roughly by where curves intersect the ordinate) derived from VL rock counts. Rocks greater than ~0.04 m in diameter were counted in roughly 70° sectors of panoramas within 10 m of the lander at Mission Success (1,089 rocks in 56.9 m^2 area from 0° to 76°), Legacy (426 rocks in 58 m^2 area from 318° to 28°) and Bonneville (689 rocks in 84.1 m^2 area from 255° to 353°). Rocks in the panoramas were manually identified using an interactive Graphic User Interface of RockIT, a component of the OASIS software (Onboard Autonomous Science Investigation System)[39]. Range data were then used to calculate apparent width (1.33 times the diameter[28]) and height. A rock of apparent width 5 cm is easily resolved at 10 m by Pancam (~18 pixels wide)[25], so that errors associated with these measurements[28] are not important on the log–log plot.

Radar

Radar reflectivity values of 0.05 and 0.04 evaluated before landing[1] indicated surfaces with loosely constrained, but reasonable, bulk densities of ~1,500 and ~1,200 kg m^{-3} at Meridiani and Gusev, respectively, that pose no special problem to landing or roving[19] and are similar to the range of bulk densities of soils that were successfully landed on and roved over by Mars Pathfinder[32]. Preliminary processing of later near-nadir 3.5-cm backscatter data with much higher spatial resolution (5 km × 5 km versus 10 km × 150 km) yield somewhat lower reflectivities of 0.02 ± 0.01 at both landing sites[33], which might be due to Doppler- and range-aliasing into the near-nadir quasi-specular echo that produces an elevated apparent noise level and reduced reflectivity. In any case, load-bearing surfaces have been confirmed by the successful landing and roving at the two sites.

The r.m.s. slope or roughness derived using the Hagfors model[34,35] indicated a smoother surface at Meridiani than at MPF (3.5-cm r.m.s. 1.4° versus 4.5°) and a smoother surface at Gusev than at VL1 (12.6-cm r.m.s. 1.7° versus 6°)[1]. Interpretation of radar data predicted that Meridiani Planum would be much less rocky and smoother than the VL2 site, and that the Gusev crater would have a combination of roughness at decimetre scales similar to or greater than VL1 and MPF sites, but would be smoother at metre scales[1]. These predictions appear consistent with the very flat, rock-free plain at Meridiani and the generally smooth, moderately rocky surface at the Gusev crater, where r.m.s. slopes from Front Hazcam stereo pairs average 3° at a 3-m scale for both rovers, but average about 30° for Spirit and 20° for Opportunity at a 10-cm scale.

Results

The close correspondence between surface characteristics inferred from orbital remote sensing data and that found at the landing sites argues that future efforts to select safe landing sites will be successful. Linking the five landing sites to their remote sensing signatures suggests that they span many of the important, probably safe surfaces available for landing on Mars, which have moderate to high thermal inertia with low to high albedo (but not low albedo and low thermal inertia). Our results show that basic engineering parameters important for safely landing spacecraft such as elevation, atmospheric profile, bulk density, rock distribution and slope can be adequately constrained using available and targeted remote sensing data.

In contrast to accurately defining the important physical characteristics of the surface, geological interpretations of the sites were less successful with respect to addressing the main scientific objectives of the mission (preserving evidence of an aqueous environment). The TES haematite signature and the geological setting of Meridiani inferred from THEMIS did correctly predict the origin of the haematite as a low-temperature precipitate[6] and the discovery of sulphate evaporites formed in an ancient aqueous environment[36]. However, the cratered plains inside Gusev do not appear to be sedimentary rocks deposited in a crater lake fed by Ma'adim Vallis, but instead appear to be a volcanic (basalt) surface that has been dominated by impact and eolian activity[37,38]. This demonstrates the uncertainty in predicting precisely what geologic materials will be available for study at landing sites from remotely sensed data.

1. Golombek, M. P. *et al.* Selection of the Mars Exploration Rover landing sites. *J. Geophys. Res.* **108**(E12), 8072, doi:10.1029/2003JE002074 (2003).
2. Cabrol, N. A., Grin, E. A. & Landheim, R. Ma'adim Vallis evolution: geometry and models of discharge rate. *Icarus* **132**, 362–377 (1998).
3. Kuzmin, R., *et al.* Geologic map of the MTM-15182 and MTM-15187 quadrangles, Gusev crater-Ma'adim Vallis region, Mars. *US Geol. Surv. Map I-2666* (US Geological Survey, Washington DC, 2000).
4. Arvidson, R. E. *et al.* Mantled and exhumed terrains in Terra Meridiani, Mars. *J. Geophys. Res.* **108**(E12), 8073, doi:10.1029/2002JE001982 (2003).
5. Christensen, P. R. *et al.* Morphology and composition of the surface of Mars: Mars Odyssey THEMIS results. *Science* **300**(5628), 2056–2061 (2003).
6. Christensen, P. R. & Ruff, S. W. Formation of the hematite-bearing unit in Meridiani Planum: evidence for deposition in standing water. *J. Geophys. Res.* **109**, E08003, doi:10.1029/2003JE002233 (2004).

7. Arvidson, R. E. *et al.* Localization and physical properties experiments conducted by Spirit at Gusev crater. *Science* **305,** 821–824 (2004).
8. Arvidson, R. E. *et al.* Localization and physical properties experiments conducted by Opportunity at Meridiani Planum. *Science* **306,** 1730–1733 (2004).
9. Kass, D. M. *et al.* Analysis of atmospheric mesoscale models for entry, descent, and landing. *J. Geophys. Res.* **108(**E12), 8090, doi:10.1029/2003JE002065 (2003).
10. Magalhaes, J. A., Schofield, J. T. & Seiff, A. Results of the Mars Pathfinder atmospheric structure investigation. *J. Geophys. Res.* **104,** 8943–8956 (1999).
11. Smith, M. D. Interannual variability in TES atmospheric observations of Mars during 1999–2003. *Icarus* **167,** 148–165 (2004).
12. Smith, D. E. *et al.* Mars Orbiter Laser Altimeter (MOLA): Experiment summary after the first year of global mapping of Mars. *J. Geophys. Res.* **106,** 23689–23722 (2001).
13. Crisp, J. A. *et al.* Mars Exploration Rover mission. *J. Geophys. Res.* **108(**E12), 8061, doi:10.1029/2002JE002038 (2003).
14. Christensen, P. R. & Moore, H. J. in *Mars* (eds Kieffer, H. H. *et al.*) 686–727 (Univ. Ariz. Press, Tucson, 1992).
15. Christensen, P. R. The spatial distribution of rocks on Mars. *Icarus* **68,** 217–238 (1986).
16. Mellon, M. T., Jakosky, B. M., Kieffer, H. H. & Christensen, P. R. High-resolution thermal inertia mapping from the Mars Global Surveyor Thermal Emission Spectrometer. *Icarus* **148,** 437–455 (2000).
17. Kieffer, H. H. *et al.* Thermal and albedo mapping of Mars during the Viking Primary Mission. *J. Geophys. Res.* **82,** 4249–4291 (1977).
18. Fergason, R. L. & Christensen, P. R. Thermal inertia using THEMIS infrared data. *Lunar Planet. Sci. XXIV* abstr. 1785 (CD-ROM, Lunar and Planetary Institute, Houston, 2003).
19. Golombek, M. P. *et al.* Selection of the Mars Pathfinder landing site. *J. Geophys. Res.* **102,** 3967–3988 (1997).
20. Presley, M. A. & Christensen, P. R. Thermal conductivity measurements of particulate materials. 2. Results. *J. Geophys. Res.* **102,** 6551–6566 (1997).
21. Herkenhoff, K. E. *et al.* Textures of the soils and rocks at Gusev crater from Spirit's Microscopic Imager. *Science* **305(**5685), 824–826 (2004).
22. Christensen, P. R. *et al.* Initial results from the Mini-TES experiment in Gusev crater from the Spirit rover. *Science* **305(**5685), 837–842 (2004).
23. Moersch, J. E., *et al.* Comparison of orbital infrared observations and surface measurements by the Mars Exploration Rover Spirit at Gusev crater. *Lunar Planet. Sci. XXXVI* abstr. 2020 (CD-ROM, Lunar and Planetary Institute, Houston, 2005).
24. Herkenhoff, K. E. *et al.* Evidence for ancient water on Meridiani Planum from Opportunity's Microscopic Imager. *Science* **306,** 1727–1730 (2004).
25. Bell, J. F. III *et al.* Pancam multispectral imaging results from the Spirit rover at Gusev crater. *Science* **305(**5685), 800–806 (2004).
26. Ruff, S. W. & Christensen, P. R. Bright and dark regions on Mars: Particle size and mineralogical characteristics based on Thermal Emission Spectrometer data. *J. Geophys. Res.* **107(**E12), 5127 doi:10.1029/2001JE001580 (2002).
27. Bell, J. F. *et al.* Pancam multispectral imaging results from the Opportunity rover at Meridiani Planum. *Science* **306,** 1703–1709 (2004).
28. Golombek, M. *et al.* Rock size-frequency distributions on Mars and implications for MER landing safety and operations. *J. Geophys. Res.* **108(**E12), 8086, doi:10.1029/2002JE002035 (2003).
29. Shepard, M. K. *et al.* The roughness of natural terrain: A planetary and remote sensing perspective. *J. Geophys. Res.* **106,** 32777–32795 (2001).
30. Anderson, F. S. *et al.* Analysis of MOLA data for the Mars Exploration Rover landing sites. *J. Geophys. Res.* **108(**E12), 8084, doi:10.1029/2003JE002125 (2003).
31. Kirk, R. *et al.* High-resolution topomapping of candidate MER landing sites with Mars Orbiter Camera narrow angle images. *J. Geophys. Res.* **108(**E12), 8088, doi:10.1029/2003JE002131 (2003).
32. Moore, H. J. *et al.* Soil-like deposits observed by Sojourner, the Pathfinder rover. *J. Geophys. Res.* **104,** 8729–8746 (1999).
33. Larsen, K. W., Haldemann, A. F. C., Jurgens, R. F. & Slade, M. A. Radar observations of recent Mars landing sites. *Lunar Planet. Sci. XXXV* abstr. 1050 (Lunar and Planetary Institute, Houston, 2004).
34. Hagfors, T. Backscattering from an undulating surface with applications to radar returns from the Moon. *J. Geophys. Res.* **69,** 3779–3784 (1964).
35. Evans, J. V. & Hagfors, T. *Radar Astronomy* 620 (McGraw-Hill, New York, 1968).
36. Squyres, S. W. *et al.* In-situ evidence for an ancient aqueous environment on Mars. *Science* **306,** 1709–1714 (2004).
37. Grant, J. A. *et al.* Surficial deposits at Gusev crater along Spirit rover traverses. *Science* **305,** 807–810 (2004).
38. Squyres, S. W. *et al.* The Spirit rover's Athena science investigation at Gusev crater, Mars. *Science* **305,** 794–799 (2004).
39. Castaño, R., *et al.* Autonomous onboard traverse science system. *Proc. 2004 IEEE Aerospace Conf. (Big Sky, Montana, March 2004)* abstr. 1375 (Institute of Electrical and Electronics Engineers, New York, NY, 2004).

Acknowledgements We are deeply indebted to the MER engineers for offering us the opportunity to test our landing site predictions with data from the surface of Mars. We acknowledge the contributions of R. Blanchard, P. Withers and the MER Atmospheric Advisory Team to the interpretations of the atmospheric entry information. M. Wyatt provided the THEMIS thermal inertia image. R. Castano, A. Castano, B. Bornstein and R. C. Anderson developed OASIS, R. Deen provided panoramas and associated range at correct resolution, and T. Stough and M. Judd provided rock counts. Research described in this paper was done by the MER project, Jet Propulsion Laboratory, California Institute of Technology, under a contract with the National Aeronautics and Space Administration.

Author Information Reprints and permissions information is available at npg.nature.com/reprintsandpermissions. The authors declare no competing financial interests. Correspondence and requests for materials should be addressed to M.P.G. (mgolombek@jpl.nasa.gov).